Original Article
pISSN 1738-2637 / eISSN 2288-2928
J Korean Soc Radiol 2018;78(1):22-29
https://doi.org/10.3348/jksr.2018.78.1.22

대한영상의학회지

Comparison of Metal Artifact Reduction for Orthopedic Implants versus Standard Filtered Back Projection: Value of Postoperative CT after Hip Replacement

정형외과 임플란트용 금속 인공물 감소법 적용 CT 영상과 표준 여과 후 역투영적용 CT 영상의 비교: 고관절치환술 환자의 수술 후 CT 영상의 가치

Jiwon Rim, MD, Jung-Ah Choi, MD*, Seun Ah Lee, MD, Eun Kyung Khil, MD
Department of Radiology, Hallym University Dongtan Sacred Heart Hospital, Hwaseong, Korea

Purpose: To evaluate Metal Artifact Reduction for Orthopedic Implants (O-MAR, Philips Healthcare) technique compared with standard filtered back projection (SFBP) technique on post-operative hip CT regarding image noise reduction and detection of post-operative complications.
Materials and Methods: Fifty-six hip CT scans after hip replacement with SFBP technique and O-MAR application were retrospectively reviewed. Region of interests (ROIs) were drawn at levels wherein acetabular cup and femoral head were largest at anterior and posterior acetabula, gluteus maximus muscle, subcutaneous fat adjacent to gluteus maximus muscle, and in area adjacent to prosthesis stem wherein lesser trochanter is largest. Hounsfield units (HU) were measured to evaluate artifact quantitatively; mean and standard deviations (SDs) calculated and compared. Periprosthetic complications were evaluated, and visibility rated between two reconstruction techniques; 1-SFBP better, 2–SFBP same as O-MAR, 3–O-MAR better.
Results: Average HU was significantly lower in O-MAR at posterior acetabulum, gluteus maximus muscle, and subcutaneous fat ($p < 0.05$). SD for HU was significantly lower in O-MAR at all ROIs ($p < 0.05$). Mean visibility of periprosthetic complications was 2.0, so equivalent.
Conclusion: Reconstruction with O-MAR technique in post-operative hip CT scans after hip replacement yielded statistically significant decrease in image noise. However, visibility of periprosthetic complications was not impacted by reconstruction technique.

Index terms
Tomography, X-ray Computed
Metals
Artifacts
Prosthesis
Hip

Received June 8, 2017
Revised August 2, 2017
Accepted September 21, 2017
***Corresponding author:** Jung-Ah Choi, MD
Department of Radiology, Hallym University Dongtan Sacred Heart Hospital, 7 Keunjaebong-gil, Hwaseong 18450, Korea.
Tel. 82-31-8086-2580 Fax. 82-31-8086-2584
E-mail: jachoi88@gmail.com

INTRODUCTION

Prosthetic hip replacement surgery is a relatively safe procedure, but there are post-operative complications. Even though complication rates are low, there are many total hip implant treatments, so radiologists commonly encounter CT images of patients with hip replacement surgery and periprosthetic complications in daily practice (1-4).

On CT, metallic hip prostheses can cause severe artifacts, limiting evaluation of anatomic structures near the metal, impair diagnostic confidence, and potentially prevent detection of complications. There are standard metal artifact reduction techniques applied to image acquisition and reconstruction (5). But artifacts exist, particularly in presence of large amounts of metallic hardware, such as total joint arthroplasties.

Currently, the most commonly used CT image reconstruction algorithm is filtered back projection. Standard filtered back projection (SFBP) is an analytic reconstruction algorithm that as-

sumes acquired projection data are without noise (6). And application of SFBP in the presence of sharp gradients in sonogram data is one source of metal artifact (7). New metal artifact reduction techniques have recently been introduced by several CT vendors. They use either single-energy or dual-energy method, and these techniques reveal promise in further reducing artifact and improving detection of pathologic lesions (7-10).

Improvement of image quality using Metal Artifact Reduction for Orthopedic Implants (O-MAR) technique (Philips Healthcare, Cleveland, OH, USA) in patients and phantom models with metallic implants and improvement on visualization of pelvic organs has been documented in literature (11, 12). However, there is concern that metal reduction techniques may not provide accurate attenuation values near hardware and may impair lesion detection by smoothing interfaces in attempts to reduce noise. And yet clinical aspects of improvement in diagnostic accuracy associated with visualization of periarticular soft tissue in pelvic CT with total hip replacement have not been directly evaluated in literature.

The purpose of this study was to evaluate value of O-MAR technique compared with SFBP technique on post-operative hip CT regarding image noise and detection of complications adjacent to metallic hip arthroplasties.

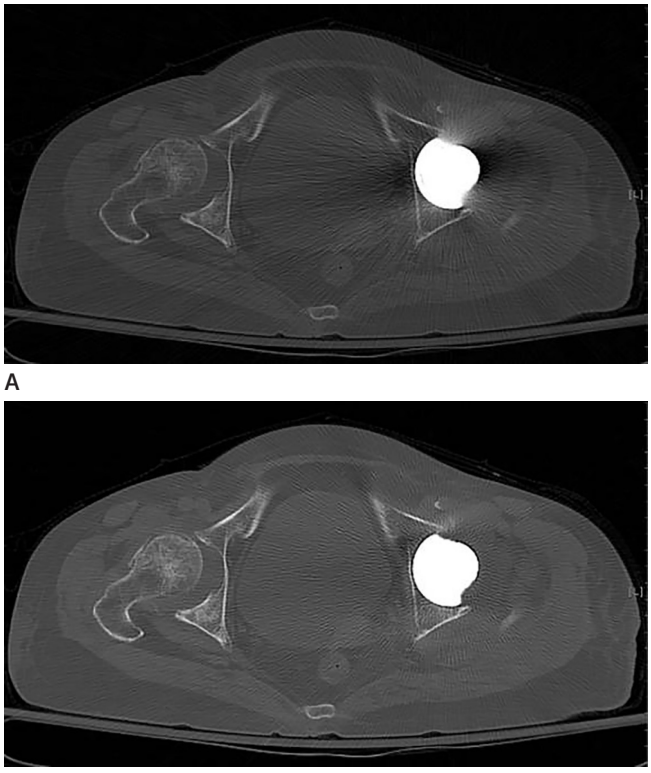

Fig. 1. Axial CT images are reconstructed using SFBP **(A)** technique and O-MAR **(B)** technique, and periprosthetic structures are obscured by streak artifact on SFBP image **(A)** but is clearly visualized on O-MAR image **(B)**.
O-MAR = Metal Artifact Reduction for Orthopedic Implants, SFBP = standard filtered back projection

MATERIALS AND METHODS

Patient Selection

Fifty-six post-operative hip CT scans (6 men and 50 women; mean age, 73.9; age range, 27–101, 53 unilateral and 3 bilateral) with SFBP technique and O-MAR application were prospectively collected January 2013-March 2014 and retrospectively reviewed (Fig. 1). Forty-three total hip replacement arthroplasty and 16 bipolar hemiarthroplasty cases were evaluated for quantitative evaluation of artifacts.

This study received Institutional Review Board (B-1208-168-010) approval. Written informed consent was waived because CT studies were clinically indicated and retrospective review of images did not require patients' informed consent.

Acquisition Protocol

Post-operative scans were obtained with a multi-detector CT (iCT 256 slice scanner; Philips Healthcare, Cleveland, OH, USA) using routine clinical technique for 3-dimension pelvis/hip CT. Scanning parameters were single-source CT acquisition, 64 × 0.625 mm detector collimation, tube voltage of 120 kVp, and tube current of 300 mAs, gantry rotation time of 0.5 seconds. Reconstruction field of view was set to 500 mm, with pixel matrix of 512 × 512. Axial slices with thickness of 3 mm with 2 mm interval and 2 mm with 1mm interval (thin data), coronal and sagittal slices with thickness of 3 mm with 3 mm interval were reformatted. No intravenous or oral contrast was used. Images were reconstructed with a SFBP algorithm with and without O-MAR (additional axial slices of 3 mm thickness).

Imaging Interpretation

SFBP and O-MAR images of each patient were separated into two different image sets and placed in different random order for each reader. Two readers were therefore blinded to both patient and reconstruction technique. Readings were conducted

over a two-week period and blinded readers measured Hounsfield units (HU) and searched for pathologic findings adjacent to the arthroplasty in each data set. Readers could scroll through images. Bone and bone-metal interfaces were evaluated in standard bone window settings (width, 2000 HU; level, 500 HU), and soft-tissue structures were evaluated in standard soft-tissue window settings (width, 350 HU; level, 50 HU).

Quantitative and Qualitative Evaluation

Image quality was assessed quantitatively by measuring mean attenuation within a region of interest (ROI) (Fig. 2). Five structures in the hip were evaluated wherein there is maximal streak artifact. ROIs were drawn on an axial image at levels wherein acetabular cup and femoral head were largest at anterior and posterior acetabula, gluteus maximus muscle, subcutaneous fat adjacent to gluteus maximus muscle, and in areas adjacent to the prosthesis stem wherein the lesser trochanter is largest, and each ROI was fully contained within the tissue measured (Fig. 3). HUs were measured in these ROIs and mean and standard deviations (SDs) calculated and compared. Image quality was assessed by two radiologists with one and four years of experience. Patient-identifying information was removed from SFBP and O-MAR images. Periprosthetic complications were evaluated for all cases and visibility compared between the two reconstruction techniques. Visibility of periprosthetic complications was evaluated as follows: 1-SFBP better, 2-SFBP same as O-MAR, 3-O-MAR better. Abnormalities were analyzed on axial images and, if present, were rated for visibility of periprosthetic complications by using the same scoring system described previously. If there was disagreement in scoring of visibility, two readers discussed to give a consensus score.

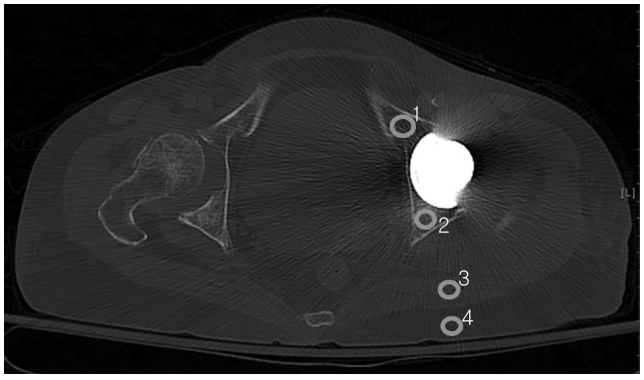

Fig. 2. Attenuations are measured on postoperative CT scans with standard filtered back projection technique by placing region of interests (circles) within anterior (1) and posterior (2) acetabula, gluteus maximus muscle (3), subcutaneous fat (4) adjacent to gluteus maximus muscle wherein there is maximal streak artifact on an axial image at the levels where acetabular cup and femoral head are largest.

Statistical Analysis

Mean attenuations at each ROI measured on SFBP and O-MAR images were compared using a paired Student t test. Wilcoxon signed rank test was used to compare SDs of HU. p-value < 0.05 was accepted as statistically significant. We used SPSS version

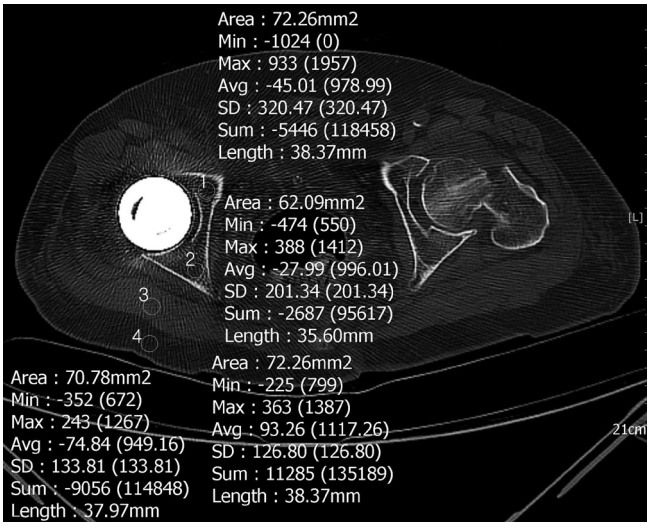

A

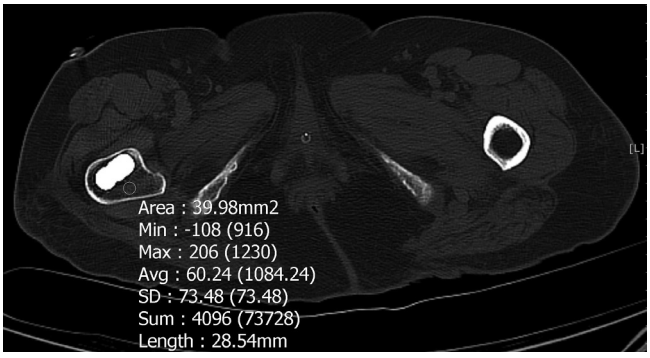

B

Fig. 3. Post-operative CT scans with Metal Artifact Reduction for Orthopedic Implants technique of an 81-year-old female patient with right bipolar hemiarthroplasty.
A. Attenuations are measured on post-operative CT scans by placing ROIs (circles) within anterior (1) and posterior (2) acetabula, gluteus maximus muscle (3), subcutaneous fat (4) adjacent to gluteus maximus muscle on axial image at levels wherein acetabular cup and femoral head are largest, and each ROI was fully contained within tissue being measured.
B. Attenuation is measured on postoperative CT scans by placing ROIs (circle) within areas adjacent to the prosthesis stem wherein the lesser trochanter is largest, and each ROI was fully contained within tissue being measured.
ROI = region of interests

21.0 (IBM Corp., Armonk, NY, USA) software for statistical analysis.

RESULTS

Average HU at posterior acetabulum was 179.10 (range, 5.47–334.59) vs. 86.78 (-21.33–275.94) for SFBP vs. O-MAR, respectively ($p < 0.001$), and gluteus maximus muscle 83.82 (3.16–191.72) vs. 60.20 (4.33–101.74) ($p = 0.034$), subcutaneous fat -60.30 (-92.95–62.75) vs. -75.75 (-113.10–-6.78) ($p = 0.007$), so significantly lower in O-MAR (Fig. 3). SD for HU was 306.23 (97.15–520.78) vs. 261.36 (72.17–499.89) ($p = 0.005$) at anterior acetabulum, 251.35 (76.71–459.65) vs. 215.88 (59.06–402.18) ($p = 0.007$) at posterior acetabulum, 134.87 (36.94–282.62) vs. 105.48 (37.88–212.57) ($p = 0.001$) at gluteus maximus muscle, and 112.46 (19.99–228.83) vs. 87.37 (18.67–151.26) ($p = 0.003$) at subcutaneous fat, and 275.04 vs. 214.76 ($p = 0.001$) at stem level (Table 1). Periprosthetic fluid collection ($n = 1$), loosening ($n = 2$), osteolysis ($n = 1$), periprosthetic fracture ($n = 1$), hardware breakage ($n = 1$) were detected on CT as postoperative complications (Fig. 4). Mean visibility of periprosthetic complications was 2.0, so equivalent in all SFBP and O-MAR images of each patient.

DISCUSSION

Metal artifact reduction (MAR) techniques have been revealed to improve image quality in patients with metallic implants (13). One of the new techniques using single-energy method is the O-MAR technique, compared with SFBP in this study. O-MAR creates a metal only image and a tissue classified image by segmenting input image into tissue and non-tissue pixels. Tissue classified sonogram is subtracted from the original image sonogram, producing an error sonogram and replacing data in the metal by interpolating values that will simulate tissue in place of the metal, removing metal data point in sonogram. Metal sonogram data is used as a mask to remove all non-metal data points from the error sonogram. This error sonogram data is back projected to generate the correction image. O-MAR uses an iterative loop wherein output correction image is subtracted from the original input image. The resultant image can become the new input image and the process can be repeated (8-10).

Many studies have revealed decreased artifact and improved subjective image quality of soft-tissue structures near metallic prosthesis using commercially available techniques. These studies have focused on patients with hip arthroplasties and other types of hardware including shoulder arthroplasties, dental hardware, fracture fixation hardware, and spinal hardware (4, 7,

Table 1. Standard Deviation for HU (O-MAR vs. SFBP)

ROI location	SFBP	O-MAR	*p*-Value
Anterior acetabulum	306.23	261.36	0.005
Posterior acetabulum	251.35	215.88	0.007
GM	134.87	105.48	0.001
Subcutaneous fat adjacent to GM	112.46	87.37	0.003
Subcutaneous fat at stem level	275.04	214.76	0.001

GM = gluteus maximus muscle, HU = Hounsfield units, O-MAR = Metal Artifact Reduction for Orthopedic Implants, ROI = region of interest, SFBP = standard filtered back projection

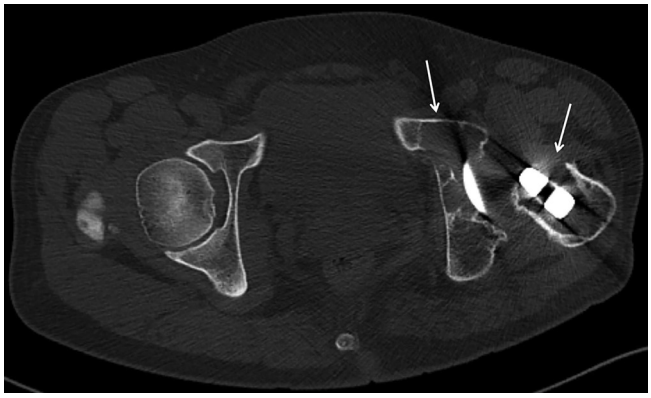

A

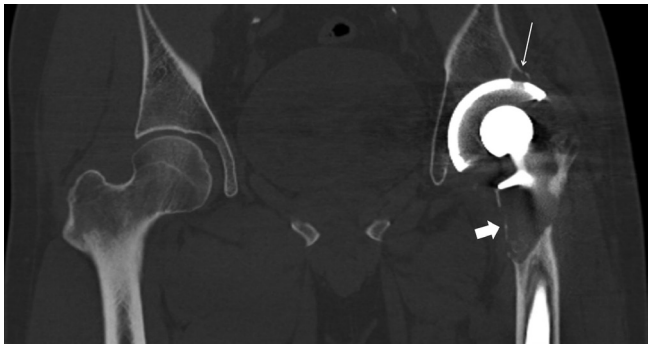

B

Fig. 4. A 47-year-old male with complications after left total hip replacement arthroplasty.
A. Axial CT image with standard filtered back projection technique shows a loosening with osteolysis at left acetabulum and around proximal stem (arrows).
B. There is wearing at superior aspect of polyethylene liner on coronal CT image with Metal Artifact Reduction for Orthopedic Implants technique (long arrow). Loosening with osteolysis around proximal stem is noted (short arrow).

8, 14-21). Several previous studies reported increase in detection rate of periarticular lesions with more confidence in analysis of these anomalies by use of MAR algorithm (22). But to our knowledge, clinical significance of these techniques has not been validated (23-25).

The purpose of this study was to compare the O-MAR technique with the SFBP technique quantitatively and qualitatively, in terms of noise and image quality near hip arthroplasty, respectively. Differences of averaged SD between O-MAR and SFBP images were highly significant for anterior acetabulum, posterior acetabulum, gluteus maximus muscle, subcutaneous fat, and at stem level. Lower SD of HU in ROIs means quantitatively homogeneous distribution of CT attenuation and could be interpreted as lower noise in selected ROI. Study results revealed that quantitative measurement of image noise induced by metallic orthopedic prostheses, expressed as averaged SD of CT numbers, can be substantially reduced by application of the O-MAR algorithm in clinical study. Reduction of image noise by use of the O-MAR algorithm was statistically significant. Study results demonstrate superiority of O-MAR technique compared with SFBP technique on post-operative hip CT regarding image noise. Results from this study support previous research results in terms of image noise (9, 26, 27).

In addition, visibility of pathologic lesions near arthroplasty implant was assessed in this study. Artifacts may be a major source of false-negative findings by obscuring soft tissue near a metallic prosthesis on post-operative CT. So, we hypothesized that decreased image noise by use of the O-MAR algorithm may improve diagnostic performance and confidence in detecting pathologic lesions near arthroplasties. Mean visibility of periprosthetic complications was equivalent in all cases, so there was equivalent value between O-MAR and SFBP images in terms of detection of complications. We attribute this result to the possibility that experienced radiologists are trained to detect periprosthetic soft tissue complication in hip arthroplasty on SFBP images despite metal artifact.

Several drawbacks of the MAR technique must be acknowledged. Information loss can occur, nonetheless, this has no impact on diagnostic quality of CT images and has not impacted diagnostic performance. Use of the O-MAR algorithm may create new artifacts as other MAR techniques, due to inaccuracies in the segmentation and classification of metal and non-metal tissue during MAR processing steps (28-30). Artifacts related to O-MAR appear as artificial dark or bright shading on corrected images. The software vendor strongly recommends cross-referenced review of CT images with and without O-MAR to prevent potential negative effect of O-MAR–related artifacts at image interpretation (7). The vendor expects that this limitation can be overcome by incorporating new adaptive correction algorithm into the current software version (9, 28).

There are several limitations to this study.

First limitation is the relatively limited number of subjects. More extensive data with larger number of subjects increases statistical power. It is possible that a larger study sample would have allowed us to demonstrate statistically significant improvement in diagnosis of periprosthetic complications with O-MAR image compared to SFBP image.

Second, there may have been recall bias because same cases O-MAR images and SFBP images were read twice. The same case presented side-by-side with a possible bias towards better scoring for CT images with O-MAR in qualitative analysis. This bias was minimized by having readers blinded to the technique and by using random reading order.

Third, pre-operative CT attenuation value near hip prostheses was not measured, so we do not know HUs of pelvic structures where there is no artifact. Change of post-operative HU may have impacted O-MAR and SFBP images; therefore, overall results would not have been impacted (8).

Although pathologic aspects of structures evaluated were found in several cases analyzed, the lack of a gold standard precluded evaluation of the diagnostic performance of the O-MAR algorithm.

Our study population had either total hip replacement arthroplasty or bipolar hemiarthroplasty. There may be image quality difference between prostheses types, total hip replacement arthroplasty and bipolar hemiarthroplasty, but the influence of prostheses types in artifact reduction was not assessed.

In addition, the HU of acetabulum is significantly impacted by patient's bone quality. So, if patient has bone density altering disease such as osteopenia or osteoporosis, measurement of acetebulum could not be representative of the whole skeleton.

Another limitation is that intra- and inter-observer agreements were not analyzed in this study.

Last, this study did not evaluate benefits of O-MAR when

scanning at lower energies that are increasingly being used for other body parts' CT scan. The simplest way of reducing metallic artifact noise is to increase tube voltage because higher-energy x-ray beams penetrate metal (10, 31, 32); however, this approach inevitably increases radiation exposure of patients. Theoretically, the benefit of O-MAR over SFBP should be the same regardless of tube voltage.

In conclusion, reconstructions using O-MAR technique in post-operative hip CT scans yielded significantly decreased image noise near hip arthroplasties as compared with SFBP technique. Evaluation of periprosthetic complication can be hindered by artifacts related to metallic hardware. However, even though CT images with O-MAR technique yielded more decreased image noise on soft tissues in patients with hip arthroplasty, the diagnosis of periprosthetic complications was not significantly different between reconstruction techniques in this study. Therefore, clinical value of O-MAR technique remains for further investigation.

REFERENCES

1. Miller TT. Imaging of hip arthroplasty. *Eur J Radiol* 2012;81:3802-3812
2. Roth TD, Maertz NA, Parr JA, Buckwalter KA, Choplin RH. CT of the hip prosthesis: appearance of components, fixation, and complications. *Radiographics* 2012;32:1089-1107
3. Cahir JG, Toms AP, Marshall TJ, Wimhurst J, Nolan J. CT and MRI of hip arthroplasty. *Clin Radiol* 2007;62:1163-1171; discussion 1172-1173
4. Gondim Teixeira PA, Meyer JB, Baumann C, Raymond A, Sirveaux F, Coudane H, et al. Total hip prosthesis CT with single-energy projection-based metallic artifact reduction: impact on the visualization of specific periprosthetic soft tissue structures. *Skeletal Radiol* 2014;43:1237-1246
5. Lee MJ, Kim S, Lee SA, Song HT, Huh YM, Kim DH, et al. Overcoming artifacts from metallic orthopedic implants at high-field-strength MR imaging and multi-detector CT. *Radiographics* 2007;27:791-803
6. Willemink MJ, de Jong PA, Leiner T, de Heer LM, Nievelstein RA, Budde RP, et al. Iterative reconstruction techniques for computed tomography part 1: technical principles. *Eur Radiol* 2013;23:1623-1631
7. Metal Artifact Reduction for Orthopedic Implants (O-MAR). White paper. Philips CT Clinical Science, Philips Healthcare. Available at: clinical.netforum.healthcare.philips.com/us_en/Explore/White-Papers/CT/Metal-Artifact-Reduction-for-Orthopedic-Implants-(O-MAR). Accessed Aug 20, 2017
8. Subhas N, Polster JM, Obuchowski NA, Primak AN, Dong FF, Herts BR, et al. Imaging of arthroplasties: improved image quality and lesion detection with iterative metal artifact reduction, a new CT metal artifact reduction technique. *AJR Am J Roentgenol* 2016;207:378-385
9. Jeong S, Kim SH, Hwang EJ, Shin CI, Han JK, Choi BI. Usefulness of a metal artifact reduction algorithm for orthopedic implants in abdominal CT: phantom and clinical study results. *AJR Am J Roentgenol* 2015;204:307-317
10. Gupta A, Subhas N, Primak AN, Nittka M, Liu K. Metal artifact reduction: standard and advanced magnetic resonance and computed tomography techniques. *Radiol Clin North Am* 2015;53:531-547
11. Long SS, Surrey D, Nazarian LN. Common sonographic findings in the painful hip after hip arthroplasty. *J Ultrasound Med* 2012;31:301-312
12. Kalender WA, Hebel R, Ebersberger J. Reduction of CT artifacts caused by metallic implants. *Radiology* 1987;164:576-577
13. Gervaise A, Osemont B, Lecocq S, Noel A, Micard E, Felblinger J, et al. CT image quality improvement using Adaptive Iterative Dose Reduction with wide-volume acquisition on 320-detector CT. *Eur Radiol* 2012;22:295-301
14. Morsbach F, Bickelhaupt S, Wanner GA, Krauss A, Schmidt B, Alkadhi H. Reduction of metal artifacts from hip prostheses on CT images of the pelvis: value of iterative reconstructions. *Radiology* 2013;268:237-244
15. Higashigaito K, Angst F, Runge VM, Alkadhi H, Donati OF. Metal artifact reduction in pelvic computed tomography with hip prostheses: comparison of virtual monoenergetic extrapolations from dual-energy computed tomography and an iterative metal artifact reduction algorithm in a phantom study. *Invest Radiol* 2015;50:828-834
16. Wang F, Xue H, Yang X, Han W, Qi B, Fan Y, et al. Reduction of metal artifacts from alloy hip prostheses in computer tomography. *J Comput Assist Tomogr* 2014;38:828-833
17. Bongers MN, Schabel C, Thomas C, Raupach R, Notohami-

prodjo M, Nikolaou K, et al. Comparison and combination of dual-energy- and iterative-based metal artefact reduction on hip prosthesis and dental implants. *PLoS One* 2015;10:e0143584

18. Subhas N, Primak AN, Obuchowski NA, Gupta A, Polster JM, Krauss A, et al. Iterative metal artifact reduction: evaluation and optimization of technique. *Skeletal Radiol* 2014;43:1729-1735
19. Winklhofer S, Benninger E, Spross C, Morsbach F, Rahm S, Ross S, et al. CT metal artefact reduction for internal fixation of the proximal humerus: value of mono-energetic extrapolation from dual-energy and iterative reconstructions. *Clin Radiol* 2014;69:e199-e206
20. Kotsenas AL, Michalak GJ, DeLone DR, Diehn FE, Grant K, Halaweish AF, et al. CT metal artifact reduction in the spine: can an iterative reconstruction technique improve visualization? *AJNR Am J Neuroradiol* 2015;36:2184-2190
21. Morsbach F, Wurnig M, Kunz DM, Krauss A, Schmidt B, Kollias SS, et al. Metal artefact reduction from dental hardware in carotid CT angiography using iterative reconstructions. *Eur Radiol* 2013;23:2687-2694
22. Yu L, Li H, Mueller J, Kofler JM, Liu X, Primak AN, et al. Metal artifact reduction from reformatted projections for hip prostheses in multislice helical computed tomography: techniques and initial clinical results. *Invest Radiol* 2009;44:691-696
23. Lee YH, Park KK, Song HT, Kim S, Suh JS. Metal artefact reduction in gemstone spectral imaging dual-energy CT with and without metal artefact reduction software. *Eur Radiol* 2012;22:1331-1340
24. Malan DF, Botha CP, Kraaij G, Joemai RM, van der Heide HJ, Nelissen RG, et al. Measuring femoral lesions despite CT metal artefacts: a cadaveric study. *Skeletal Radiol* 2012;41:547-555
25. Verburg JM, Seco J. CT metal artifact reduction method correcting for beam hardening and missing projections. *Phys Med Biol* 2012;57:2803-2818
26. Wilson JM, Christianson OI, Richard S, Samei E. A methodology for image quality evaluation of advanced CT systems. *Med Phys* 2013;40:031908
27. Hilgers G, Nuver T, Minken A. The CT number accuracy of a novel commercial metal artifact reduction algorithm for large orthopedic implants. *J Appl Clin Med Phys* 2014;15:4597
28. A new method for metal artifact reduction in CT. International Conference in X-ray Computed Tomography, 2011. Available at: https://repository.tudelft.nl/assets/uuid:22d5815d-dcfe-48df-93a4-9d1c4e8e85fc/MS-33.229.pdf. Accessed Feb 6, 2017
29. Andersson KM, Norrman E, Geijer H, Krauss W, Cao Y, Jendeberg J, et al. Visual grading evaluation of commercially available metal artefact reduction techniques in hip prosthesis computed tomography. *Br J Radiol* 2016;89:20150993
30. Han SC, Chung YE, Lee YH, Park KK, Kim MJ, Kim KW. Metal artifact reduction software used with abdominopelvic dual-energy CT of patients with metal hip prostheses: assessment of image quality and clinical feasibility. *AJR Am J Roentgenol* 2014;203:788-795
31. Buckwalter KA, Lin C, Ford JM. Managing postoperative artifacts on computed tomography and magnetic resonance imaging. *Semin Musculoskelet Radiol* 2011;15:309-319
32. White LM, Buckwalter KA. Technical considerations: CT and MR imaging in the postoperative orthopedic patient. *Semin Musculoskelet Radiol* 2002;6:5-17

정형외과 임플란트용 금속 인공물 감소법 적용 CT 영상과 표준 여과 후 역투영적용 CT 영상의 비교: 고관절치환술 환자의 수술 후 CT 영상의 가치

임지원 · 최정아* · 이선아 · 길은경

목적: 정형외과 임플란트용 금속 인공물 감소법(Metal Artifact Reduction for Orthopedic Implants; 이하 O-MAR) 적용 CT 영상이 표준 여과 후 역투영적용 CT 영상과 비교하여 영상잡음 감소와 수술 후 합병증 발견에 도움이 되는지 평가해 보고자 하였다.

대상과 방법: 고관절 치환술 시행 후 standard filtered back projection (이하 SFBP)과 O-MAR가 적용된 CT을 얻은 환자 56명을 후향적으로 분석하였다. 관심영역은 비구컵과 대퇴골두가 가장 크게 보이는 영상에서 비구의 전방 및 후방, 인접한 대둔근 및 피하지방, 그리고 소전자가 가장 크게 보이는 영상에서 인공삽입물 근처에 위치하였다. 인공음영 정도의 평가를 위해 SFBP 적용영상과 O-MAR 적용영상에서 region of interests의 평균 Hounsfield unit (이하 HU)과 HU의 표준편차를 계산하여 차이가 있는지 비교하였다. 인공삽입물 주위 합병증을 평가하였고 그 합병증의 가시성을 두 가지 영상재구성기술에서 비교하여 다음과 같이 수치화하였다; 1- SFBP이 더 나음, 2-SFBP이 O-MAR와 동일, 3-O-MAR이 더 나음.

결과: 평균 HU값은 비구 후방, 대둔근, 피하지방에서 O-MAR 적용영상이 유의하게 낮게 나타났다($p < 0.05$). HU의 표준편차는 모두에서 O-MAR 적용영상이 유의하게 낮게 나타났다($p < 0.05$). 인공삽입물 주위 합병증의 평균 가시성은 2.0으로 두 영상재구성기술이 동등하였다.

결론: O-MAR를 적용하여 재구성된 고관절치환술 후 영상은 SFBP 적용 CT영상과 비교하여 영상 잡음이 통계적으로 의미 있게 감소함을 정량적으로 확인하였다. 반면에 인공삽입물 주위 합병증의 진단은 영상재구성기술의 차이에 영향을 받지 않았다.

한림대학교 동탄성심병원 영상의학과